

TETRAHEDRON REPORT NUMBER 247

APPLICATIONS OF ^{15}N NMR SPECTROSCOPY TO THE STUDY OF MOLECULAR STRUCTURE, STEREOCHEMISTRY AND BINDING PHENOMENA

GERALD W. BUCHANAN

Ottawa-Carleton Chemistry Institute, Department of Chemistry, Carleton University, Ottawa, Canada K1S 5B6

(Received in USA 20 April 1988)

CONTENTS

1. Introduction	581
2. Methods of Sensitivity Enhancement	582
2.1. The ^1H - ^{15}N nuclear Overhauser effect	582
2.2. The INEPT experiment	583
2.3. ^1H Detected multiple quantum coherences	583
3. Structure Determination Using ^{15}N NMR	583
3.1. Chemical shift studies in solution.	583
3.1.1. General background.	583
3.1.2. Contributions to ^{15}N chemical shifts	584
3.1.3. Substituent effects on ^{15}N chemical shifts	585
3.1.4. Functional group analysis via ^{15}N NMR	586
3.1.5. Tautomeric equilibria and protonation sites	586
3.2. The use of spin coupling constants involving nitrogen-15 in structure determination	588
4. Stereochemical Analysis	589
4.1. Conformational analysis in cyclohexanes using ^{15}N chemical shifts	589
4.2. ^{15}N Chemical shifts as a probe for steric inhibition of resonance	589
4.3. Chiral recognition using ^{15}N NMR spectroscopy	590
4.4. Conformational analysis of peptides.	590
4.5. Configurational and conformational analysis via spin coupling to ^{15}N	591
4.6. Stereochemical dynamics studied by ^{15}N NMR	593
4.7. Molecular dynamics as studied by ^{15}N T ₁ s and ^1H - ^{15}N nOes	593
5. Metal Binding Phenomena	594
5.1. Metal ion binding to nucleic acid components	595
5.2. Metal-nitrogen binding in amino acid complexes and enzymes	597
6. ^{15}N NMR Studies of Solids	598
6.1. Proton transfer kinetics via solid phase ^{15}N NMR	598
6.2. ^{15}N CPMAS studies of proteins and other biopolymers	599
6.3. ^{15}N Chemical shift tensors	601
6.4. Measurement of ^{15}N -H bond distances via solid state ^{15}N NMR	602
6.5. Characterization of surface bound species via ^{15}N NMR in solids	602

1. INTRODUCTION

The low sensitivity and low natural abundance (0.37%) of the ^{15}N nucleus have tended to retard its use in the solution of chemical problems. The ^{14}N isotope, while being 99.63% naturally abundant, suffers from the disadvantage of a quadrupole moment which normally leads to very broad linewidths

Table 1. ^{15}N at natural abundance compared to ^1H and ^{13}C

Nucleus	% Abundance	Relative sensitivity	Observation time (same S/N)
^1H	99.99	1.0	1.0
^{13}C	1.11	1.76×10^{-4}	3.2×10^7
^{15}N	0.37	3.9×10^{-6}	6.8×10^{10}

of up to 1000 Hz. Hence its potential for use in the solution of chemical problems is severely limited.

Early work in ^{15}N NMR indicated that the method possessed vast potential since the range of chemical shifts was *ca* 900 ppm. Also the ^{15}N nucleus, with spin quantum number $I = 1/2$, exhibits resonances the linewidths of which are comparable to those for ^1H and ^{13}C . Hence the major obstacle inhibiting the general application of ^{15}N NMR spectroscopy has been one of low signal intensities. To give a clear indication of this situation it is instructive to compare the theoretical situation for ^{15}N to that for ^1H and ^{13}C as depicted in Table 1. Despite these difficulties, considerable progress in the field took place in the early years.¹⁻³

Recent advances in instrumentation however, involving higher magnetic fields, cross polarization techniques and multidimensional methods have increased dramatically the sensitivity for observation of ^{15}N . Thus the range of problems now amenable to examination by natural abundance ^{15}N NMR spectroscopy has expanded to a remarkable extent.

Furthermore, the ^{15}N studies need no longer be limited to solutions, since the magic angle spinning technique has made possible high resolution spectra of solids.

It is the intent of this Report to review the applications of ^{15}N NMR to the general areas of organic structure determination, stereochemistry and binding. Most of the examples are taken from the literature since 1980, because earlier applications have been reviewed previously¹⁻³ or with a different emphasis.⁴

Before embarking on this, however, it is instructive to examine the recently reported methods of signal to noise enhancement so that the reader may have a realistic expectation with regard to the applicability of a given experimental procedure to a particular problem at hand. Some familiarity with routine Fourier transform techniques as applied to the detection of ^{15}N resonances¹⁻³ is assumed.

2. METHODS OF SENSITIVITY ENHANCEMENT

2.1. The ^1H - ^{15}N nuclear Overhauser effect

Decoupling of protons bonded to nitrogen will lead to multiplet collapse to a singlet resonance. In addition, if the mechanism of spin-lattice relaxation is uniquely dipole-dipole, then an additional increase in the ratio of signal to noise of $1/2$ ($\gamma_{\text{H}}/\gamma_{\text{N}}$) is anticipated, i.e. the well documented nuclear Overhauser effect (nOe).⁵ Since γ_{N} is negative, however, a negative signal will result. This creates no problem if there is complete dipole-dipole relaxation, however the contribution of other relaxation mechanisms can result in a near zero ^{15}N resonance intensity in unfavourable cases. This is particularly evident for non-protonated nitrogens, so that it is now common practice to employ gated ^1H decoupling methods to suppress the nOe while observing ^{15}N .

For very large or highly associated molecules, additional complications arise since the motional narrowing conditions no longer apply. Contributions from five factors have been recognized which can lead to nulling of ^1H decoupled ^{15}N signals,⁶ so that caution must always be exercised in choosing experimental conditions.

2.2. The INEPT experiment

The acronym INEPT is used to describe the experiment by which Inensitive Nuclei are Enhanced by Polarisation Transfer and was first reported by Morris⁷ for the ^1H - ^{15}N case. This experiment leads to approximately a ten-fold increase in the ^{15}N signal intensity due to the higher magnetogyric ratio of the ^1H than the ^{15}N nucleus. An additional improvement in sensitivity can result from the faster spin-lattice relaxation of the protons than for the ^{15}N , since it is the ^1H relaxation times which govern the rate at which the pulse sequence can be repeated. This method is applicable only to systems in which detectable ^1H - ^{15}N couplings exist. Subsequently, a modification of the INEPT experiment has been reported⁸ which enables one to obtain significant enhancements even for nonprotonated nitrogen resonances.

2.3. ^1H Detected multiple quantum coherences

In an exciting development, it has recently been demonstrated⁹ that for nitrogens which are spin coupled to protons, one can indirectly detect the ^{15}N resonances with the full sensitivity of the protons to which they are coupled, resulting in an enhancement of approximately 1000 over simple direct detection of ^{15}N . The technique utilizes two-dimensional $^1\text{H}/^{15}\text{N}$ shift correlation via proton detected double quantum coherence.¹⁰ In general, correlation of ^1H with ^{15}N signals presents a greater problem than with ^{13}C signals since the natural abundance of ^{15}N is *ca* 3 times lower than ^{13}C and also because the ^{15}N correlated spectra must be recorded in H_2O instead of D_2O solution. A pulse sequence must be used which suppresses ^1H signals which are not coupled to ^{15}N . Furthermore the H_2O resonance must be suppressed. Recently there has been a report¹¹ of optimal ^1H and ^{15}N pulse sequences for correlating ^1H and ^{15}N shifts in solution. The method has been applied to the protein bovine pancreatic trypsin inhibitor (BPTI). For this protein ($M_r = 6500$), a 50 mg sample was examined in 0.4 ml of 90% $\text{H}_2\text{O}/\text{D}_2\text{O}$. After 11 hr data accumulation time, a natural abundance two dimensional ^1H - ^{15}N correlated spectrum with high signal to noise ratio was obtained.

Using these methods it is clearly now feasible to examine materials of molecular weight 10^4 – 10^5 at relatively low concentrations (10^3 – 10^{-4} M) in relatively short periods of time.

3. STRUCTURE DETERMINATION USING ^{15}N NMR

3.1. Chemical shift studies in solution

3.1.1. *General background.* The single most useful parameter of structure determination remains the chemical shift. For ^{15}N , the range of chemical shifts for neutral organics spans *ca* 900 ppm, so that functional groups containing nitrogen can often be identified solely from their characteristic resonance positions. Although the literature contains data referenced to a variety of external chemical shift standards, it is now commonplace (and strongly recommended) to use the scale having the resonance for anhydrous liquid ammonia at $\delta_{\text{N}} = 0$. This is consistent with the use of TMS as the standard for both ^1H and ^{13}C chemical shifts. On this basis, increasing positive δ values are in the direction of increasing frequency, i.e. to lower fields, so that in fact these are all deshielding scales.

For practical purposes, one can employ external chemical shift reference materials such as saturated aqueous NH_4Cl , CH_3NO_2 or HNO_3 . The chemical shifts (relative to anhydrous liquid NH_3) for these and other compounds which have been employed as external standards are included in Table 2.

In Fig. 1 are presented the chemical shift ranges for the most common nitrogen containing functional groups. In view of the *ca* 900 ppm range of ^{15}N shieldings, some discussion of the present status of nitrogen chemical shift theory is necessary. Knowledge of contributing factors to ^{15}N shifts will facilitate the application of the technique to the solution of chemical problems.

Table 2. ^{15}N chemical shifts (ppm) of some common standards¹

Compound	δ_{N}	Conditions
NH_3	0.00	liquid, 25°C
	3.37	liquid, -50°C
$\text{N}^*\text{H}_4\text{NO}_3$	21.60	aqueous HNO_3 (1-10 m)
	20.68	sat'd aqueous solution
NH_4Cl	27.34	sat'd aqueous solution
$(\text{CH}_3)_4\text{NCl}$	43.54	sat'd aqueous solution
HNO_3	375.80	1M aqueous
	367.64	2M aqueous
	362.00	10M aqueous
NaNO_3	376.53	sat'd aqueous
$\text{NH}_4\text{N}^*\text{O}_3$	376.25	sat'd aqueous

3.1.2. *Contributions to ^{15}N chemical shifts.* The status of ^{15}N chemical shift theory is at approximately the same stage as that for ^{13}C NMR. One approach which is now standard involves the subdivision of contributions to the overall nuclear shielding constant, σ_{tot} , into four categories. These contributions are from the diamagnetic term, σ_d , the paramagnetic term σ_p , the anisotropic term σ_a , and the solvent term σ_s . The order of importance of these terms to the overall shielding at nitrogen is generally accepted to be $\sigma_p \geq \sigma_d \gg \sigma_a \sim \sigma_s$, however in individual cases this order may be permuted somewhat.

The diamagnetic term is directly related to electron density and can be evaluated by the Lamb formula.¹² In essence, the higher the electron density at nitrogen the more shielded (i.e. lower δ_{N}) will be the resonance, due to magnetically induced local electronic circulations about the nucleus.

For an isolated nitrogen atom, σ_p would be zero. For a nitrogen atom in a molecule, however, the electronic environment is not spherically symmetric and there will be hindrance to the diamagnetic circulations. Thus σ_p is a local correction due to the electronic environment, and corresponds to a mixing of ground state electronic contributions with low lying excited states by the applied field. One can view σ_p in terms of three structurally related contributions, as outlined in equation (1) below.

$$\sigma_p = -e^2 h^2 \langle r^{-3} \rangle_{2p} [2m^2 c^2 \Delta E]^{-1} \Sigma_B Q_{AB} \quad (1)$$

ΔE is the average electronic excitation energy and is a measure of the accessibility of low lying paramagnetic electronically excited states.

The $\langle r^{-3} \rangle$ term is the average inverse cube of the non-*s* orbital radius at nitrogen, while ΣQ represents the sum of all bond order and charge density terms for the bonding electrons at atoms *B* which are bonded to nitrogen *A*. Due to the negative sign of the σ_p contribution it is clear that a deshielded nitrogen will result if ΔE or $\langle r^{-3} \rangle$ are decreased or if ΣQ increases i.e. for a multiply bonded nitrogen.

The anisotropic term, σ_a , represents contributions from neighbouring anisotropic atoms and bonds as well as ring current effects. Since this is an internal field effect, its magnitude is expected to be the same for all nuclei (in ppm) for a given spatial orientation of the anisotropic element with respect to the magnetic nucleus under study. For protons, where the overall chemical shift range for neutral organic molecules is only *ca* 20 ppm at most, normal anisotropic contributions of a few ppm can be very important in the determination of the observed chemical shift. For nuclei such as ^{15}N however, with an overall shift range of *ca* 900 ppm these small anisotropic contributions will not normally be of substantial importance.

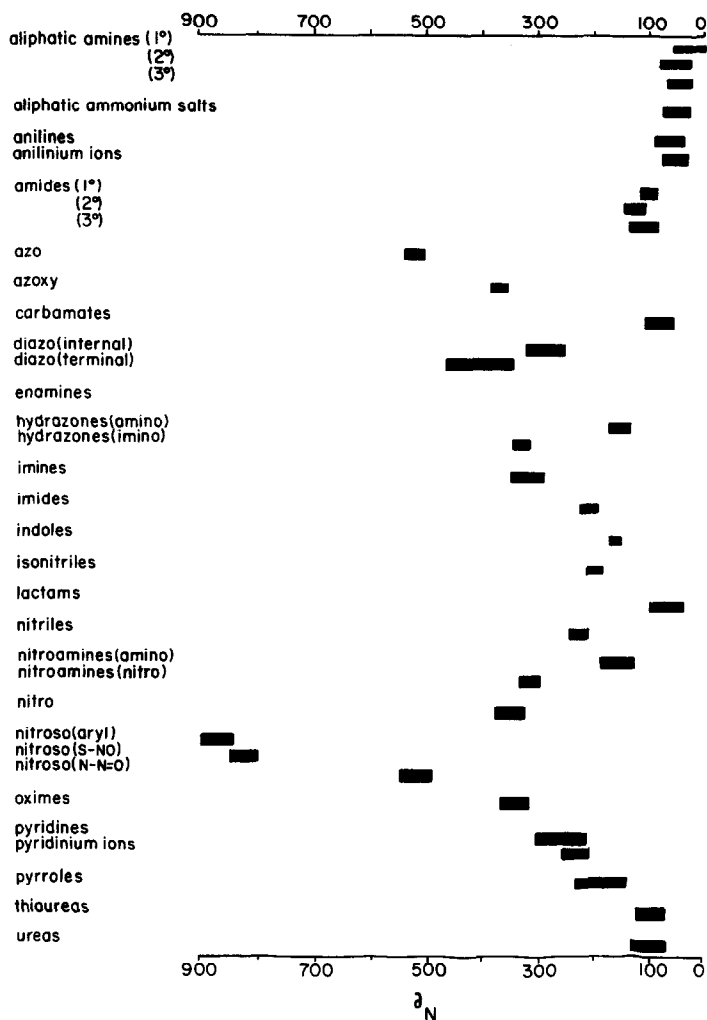


Fig. 1. ^{15}N chemical shift ranges for common functional groups.

In ^{15}N NMR there is potentially the possibility of very pronounced solvent effects on the observed chemical shifts, due to the presence of the nitrogen lone pair of electrons. In general, solvents which act as lone pair acceptors will lead to significant upfield shifts in the position of ^{15}N resonances.¹³ The underlying theoretical rationale for such a trend is probably found in the paramagnetic contribution, in that ΔE is expected to increase as a result of lone pair association and thus the magnitude of the deshielding paramagnetic term will be reduced.

3.1.3. *Substituent effects on ^{15}N chemical shifts.* In addition to the dependence of the ^{15}N chemical shift on the nature of the functionality at nitrogen, extensive studies of the influence of systematic alteration of the substituent patterns have been carried out. For example acyclic aliphatic amines display regular and systematic trends with alkyl substitution.¹⁴⁻¹⁶ In general replacement of hydrogens directly on nitrogen by alkyl groups tends to deshield the nitrogen so that additive substituent parameters may be derived¹⁵ and applied in the same way that has been extensively done in ^{13}C NMR.^{17,18}

Major downfield (deshielding effects) of 10–12 ppm result from both α and β alkyl substitution on acyclic aliphatic amines, while the γ substituent effect is a minor shielding contribution of *ca* 2 ppm.

There have been several comprehensive reviews of the systematic influence of substituents on ^{15}N shifts.¹⁻³ Accordingly such material will not be treated extensively in the present Report.

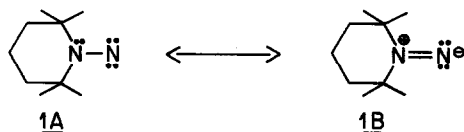
3.1.4. *Functional group analysis via ^{15}N NMR.* The utility of ^{15}N chemical shifts for functional group characterization has been illustrated in the examination of the 1,1-diazene (N-nitrene) intermediate **1** shown below.¹⁹



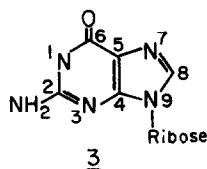
The 1,1-diazene system is considerably less stable than the 1,2-diazene counterparts (azo compounds) of general structure **2**. Due to the limited stability of the 1,1-isomers the ^{15}N spectra have been recorded at -90°C . Assignment of the resonances was unambiguous due to the availability of both singly and doubly ^{15}N labelled material.

The chemical shift of the amino (ring) nitrogen (321.4) is consistent with an amino nitrogen the lone pair of which is highly delocalized, since it is substantially deshielded relative to normal sp^3 hybridized nitrogen resonances. In fact it has a chemical shift comparable to those of nitrones, nitrates and nitro compounds which lack nonbonding electrons on nitrogen.

For the nitrene nitrogen, the chemical shift is 917.0, which represents the most deshielded neutral nitrogen chemical shift yet reported. It has been suggested that the ΔE contribution to the paramagnetic shielding term is responsible for the observation. Experimentally a low-lying $n-\pi^*$ electronic transition, $\lambda_{\text{max}} = 543 \text{ nm}$, has been found in the UV spectrum of this molecule. This contribution to ΔE reduces the denominator in the σ_p term hence leading to an enhanced deshielding effect. On the basis of the ^{15}N chemical shifts at both nitrogens, resonance form **1B** (below) is deemed to be the major contributor to the structure of **1**.

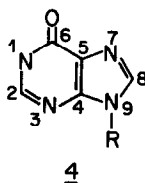


3.1.5. *Tautomeric equilibria and protonation sites.* ^{15}N NMR has proven to be particularly useful in this area, especially for the characterizations of the nitrogens of nucleosides and nucleotides. Relatively early work²⁰ was carried out on the nucleosides adenosine, guanosine, inosine, uridine, thymidine and cytidine. Complete ^{15}N chemical shift assignments were made. In addition, the protonation sites of adenosine, ATP, cytidine and guanosine as well as simpler model compounds such as pyridine were determined via ^{15}N shift changes induced by successive additions of trifluoroacetic acid (TFA). For pyridine, an upfield ^{15}N shift of 97 ppm is observed upon protonation. In the case of guanosine, **3**, the N-7 resonance shifts upfield by *ca* 40 ppm upon addition of 1 molar equivalent of TFA, indicating that this is the preferred site of protonation.



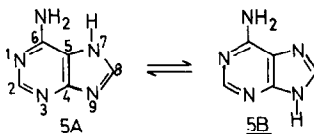
By contrast, the N-3 resonance shows only minor upfield shifts (*ca* 1 ppm) while N-9 and the NH_2 group shift downfield by *ca* 3 ppm. N-1 is essentially unaffected.

More recently²¹ similar work was done on the structurally related inosine molecule **4**, again leading to the conclusion that the N-7 site (below) is preferred for protonation.



With respect to nucleotides, the pH dependence of the ^{15}N chemical shifts of several guanosine monophosphates has been studied in detail.²² For 5'-GMP, the N-1 site begins to deprotonate at pH 8, leading to a downfield shift of 60 ppm on full deprotonation. Thus it is evident that protonation–deprotonation effects can lead to changes in ^{15}N chemical shifts of over 100 ppm.

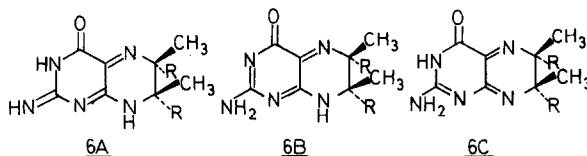
It has been demonstrated amply that ^{15}N chemical shifts also provide valuable information regarding the character of the nitrogens of the nucleic acid bases. For adenine, specific ^{15}N labelling at N1, N3, N6', N7 and N9 provided unequivocal chemical shift assignments as well as elucidation of the position of the tautomeric equilibrium.²³ Both adenine and its conjugate acid were shown to exist in solution as the N9-H tautomer **5B** (below).



Interestingly, conversion of adenine to its conjugate base ($\text{pK}_a \sim 10$) results in a downfield shift (of 56 ppm) in the N9 resonance indicating that this is the preferred deprotonation site.

It is important to note that protonation of aliphatic amines induces ^{15}N shifts which are in general *opposite* in direction to those found for sp^2 or sp hybridized nitrogen. Thus protonation of such molecules generally *deshields* the nitrogen, with the magnitude of the effect being also dependent upon solvent, concentration and counterion.¹ An exception to this trend, however, is found for diisopropyl amine where protonation shields the ^{15}N resonance by 3.5 ppm.¹⁵

In the pteridine field, the structure of the quinoid 6,7-dimethyl-7,8-dihydro-6H-pterin in aqueous solution has been in doubt.²⁴ Essentially three possible tautomeric structures, **6A**, **6B** and **6C**



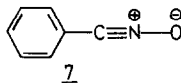
had been proposed. Based on the ^{15}N chemical shifts it was established that tautomer **6B** predominates in aqueous solution near neutral pH.

3.2. The use of spin coupling constants involving nitrogen-15 in structure determination

In this section the applicability of direct i.e. one-bond ^{15}N couplings to other magnetic nuclei for aspects of structure determination will be discussed. A later section (4.5.) will deal with the use of geminal and vicinal couplings to ^{15}N for stereochemical determinations.

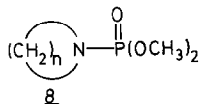
For $^1J_{\text{NH}}$, the couplings appear to be dominated by the Fermi contact mechanism and hence some correlation with the degree of *s* character in the HN bond is expected. In general this has been found to be the case with values of $^1J_{\text{NH}}$ being *ca* 75, 90 and 135 Hz for sp^3 , sp^2 and sp hybridized nitrogen respectively. In addition there are well documented effects of solvent and substituent electronegativity on these parameters which have been reviewed recently.¹

Most $^1J_{\text{NC}}$ couplings are negative in sign which again indicates that the dominant mechanism for the coupling interaction is Fermi contact. However it is now apparent²⁵ that other mechanisms are very often present leading to complications in the interpretation of the data in terms of %*s* character at nitrogen. Typically the range of absolute values for this parameter is 0–20 Hz, with the notable exception of the value of -77.5 Hz for the system **7** depicted below.¹



To summarize, although there may be useful and interesting trends in $^1J_{\text{NC}}$ in a related series of molecules, in general this parameter has very limited utility for structure elucidation.

Several reports of the use of one-bond couplings between ^{15}N and ^{31}P for structure elucidation have appeared. In a series of heterocyclic phosphoramidates (general structure depicted below) **8** the variation of $^1J_{\text{NP}}$ with ring size (Table 3) is indicative of hybridization changes in the exocyclic N–P bond.²⁶



For the 5-membered and larger rings, the $^1J_{\text{NP}}$ values are interpreted in terms of essentially complete sp^2 hybridization at nitrogen. The result for the acyclic system is consistent with this suggestion. Assuming the dominance of the Fermi contact mechanism for $^1J_{\text{NP}}$, one would expect that an increase in *s* character in the N–P bond would lead to an increased absolute value for the ^{15}N - ^{31}P coupling constant. For the case of the aziridine derivative, in any form having appreciable double bond character in the N–P bond, one would expect a substantial amount of bond angle strain in the 3-membered ring. Hence one anticipates a situation in which the hybridization at

Table 3

Ring size ($n + 1$)	$^1J(^{15}\text{N}-^{31}\text{P})$ (Hz)*
3	9.3
4	20.9
5	41.2
6	39.1
7	42.7
8	41.8
9	37.6
acyclic (diethyl)	42.2

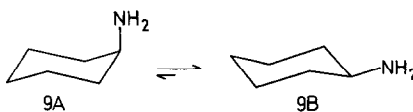
* Sign is most likely to be negative.

nitrogen is essentially sp^3 , leading to a reduction in the absolute value of the observed $^1J_{\text{NP}}$. For the 4-membered azetidine derivative an intermediate value of $^1J_{\text{NP}}$ is found indicating a state of hybridization between the extremes of sp^2 and sp^3 . These experimental results are in good agreement with results of Finite Perturbation calculations assuming dominance of the Fermi contact term.¹⁷ From this work, pure trigonal geometry at N gives a calculated $^{15}\text{N}-^{31}\text{P}$ coupling of -39 Hz, while pure pyramidal geometry gives a value of -12 Hz.

4. STEREOCHEMICAL ANALYSIS

4.1. Conformational analysis in cyclohexanes using ^{15}N chemical shifts

Relatively few applications have appeared in this area, however ^{15}N NMR has been used²⁸ to permit the first direct detection of the axial conformer (**9a**, below) of aminocyclohexane. The combination of 99.9% ^{15}N enrichment and a full nuclear Overhauser enhancement upon ^1H decoupling allowed clear detection of the axial conformer resonance after 500–800 scans at a temperature of 173 K in toluene- d_8 or CD_2Cl_2 solution.

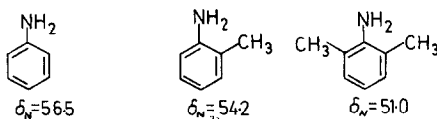


From the relative intensities of the NH_2 resonances for the axial and equatorial conformations, the conformational free energy, $-\Delta G^0$, for the NH_2 group was calculated to be 5.9 ± 0.3 kJ/mol. The resonance for the axial nitrogen is found to be shielded relative to its equatorial counterpart by 10–11 ppm. This chemical shift difference is similar to that reported previously for the model compounds *cis*- and *trans*-4-*t*-butyl-cyclohexylamine.²⁹ Thus it appears that the gauche- γ steric shift in ^{15}N NMR is of comparable magnitude to that observed in ^{13}C NMR,³⁰ and should serve as a powerful tool in stereochemical determinations.

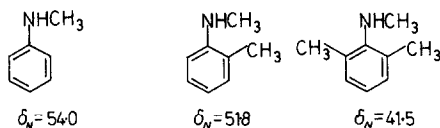
4.2. ^{15}N Chemical shifts as a probe for steric inhibition of resonance

For three series of substituted anilines ^{15}N chemical shifts have been employed to monitor steric inhibition of nitrogen lone pair delocalization into the aromatic ring.^{31–33} It has been suggested that steric inhibition should lead to shielded ^{15}N resonances due to lower contributions from resonance forms containing $\text{C}=\text{N}$ units.

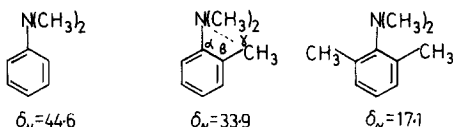
In the case of aniline itself,³¹ *ortho* methylation induces relatively minor upfield shifts at N as depicted below.



For the N-methyl aniline series,³² the first *ortho* methyl function induces only a minor upfield shift at N (2.2 ppm), while the second has a much more pronounced effect (10.3 ppm).



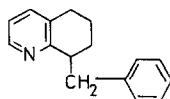
In the case of the N,N-dimethylated series,³³ the effects are much more pronounced, as indicated below.



Regardless of their origin, these steric shifts may also be regarded as further manifestations of γ -effects.

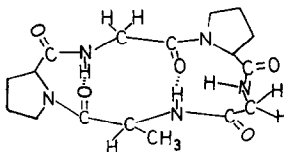
4.3. Chiral recognition using ¹⁵N NMR spectroscopy

It is now well known that chiral recognition can be achieved through the chemical shift differences observed in the diastereomeric collision complexes formed between optically active solutes and solvents. ¹H NMR has been employed primarily for this purpose.^{34,35} ¹⁵N chemical shift differences have also been utilized to this end³⁵ in the case of racemic 8-benzyl-5,6,7-tetrahydroquinoline (below) in the presence of a number of optically active acids and β -cyclodextrin. Diastereomeric ¹⁵N shifts of up to 0.66 ppm have been found in the complex with *R*-(-)-mandelic acid.



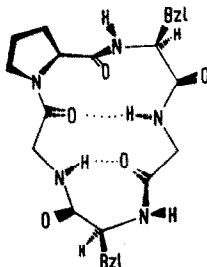
4.4. Conformational analysis of peptides

The initial indication that ¹⁵N NMR would be useful in this important area came in 1973 with the work³⁷ on ¹⁵N enriched L-Val-Gly. Subsequently strategies for study of peptides at natural abundance were illustrated³⁸ using Gramicidin S and some N-acetyl tripeptides. This was followed by work³⁹ on the cyclic pentapeptide cyclo-(Gly(1)-Pro-Gly(2)-D-Ala-Pro) (below).



The ^{15}N resonances for the three amino acids in this peptide were found to resonate over a 33 ppm range with no overlap. From specific ^{15}N labelling unambiguous assignments were made and the sensitivity of amide ^{15}N chemical shifts to solvent and conformational changes was established.

The advent of cross polarization techniques and multidimensional methods, with the concomitant increase in sensitivity has led to a plethora of applications of ^{15}N NMR in this area. For example, 2-dimensional ^1H - ^{15}N chemical shift correlation methods have been used to assign the ^{15}N resonances of a 330 mM solution of cyclo(Pro-Phe-Gly-Phe-Gly) in DMSO.⁴⁰ The magnitude of the ^1H - ^{15}N one bond coupling constants were used by analogy with earlier work,⁴¹ to deduce that all four peptide bonds are *trans* as depicted below.



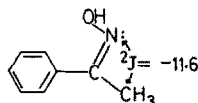
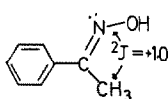
More recently, these methods as well as 2-dimensional ^1H - ^{13}C COSY experiments have led to the essentially complete spectral assignments for the linear peptide antibiotic Gramicidin A.^{42,43} This material has the structure HCO-L-Val-Gly-L-Ala-D-Leu-L-Ala-D-Val-L-Val-D-Val-L-Tryp-D-Leu-L-Tryp-D-Leu-L-Tryp-D-Leu-L-Tryp-NHCH₂CH₂OH, and is of interest because it dimerizes to form ion conducting channels in membranes.

Of the 16 nitrogens present in this molecule the ^{15}N resonances for all 16 have been resolved and 12 have been assigned unambiguously via ^1H - ^{15}N COSY. The 400 MHz ^1H spectrum of Gramicidin A is poorly resolved, but the use of both ^1H - ^{13}C and ^1H - ^{15}N COSY experiments, taking advantage of the much larger chemical shift range for both heavier nuclei, has permitted assignments of many of the ^1H resonances. Sequential assignments of the ^1H resonances in the peptide chain were then achieved via qualitative estimates of interproton distances obtained from 2-D ^1H - ^1H NOESY spectra and techniques which are now well established in the field.⁴⁴ With the ^1H spectral data in hand the magnitudes of the vicinal H—N—C—H couplings can then be employed for conformational analysis of the peptide units. In this case the occurrence of internal mobility in Gramicidin A is proposed and the presence of several conformations in solution has been suggested.

4.5. Configurational and conformational analysis via spin coupling to ^{15}N

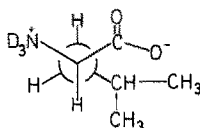
Geminal (i.e. two-bond) couplings between ^{15}N and ^1H can be employed for configurational analysis.⁴⁵ In general the geminal coupling is relatively large and negative in sign when the nitrogen lone pair is *cis* to the coupled proton, while for the *trans* orientation the coupling is small and positive in sign.

Similar trends have been found for geminal ^{13}C - ^{15}N couplings in oximes⁴⁶ and imines.⁴⁷ Results for configurationally isomeric acetophenone oximes are presented below.

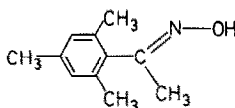


Vicinal (i.e. three bond) couplings to ^{15}N exhibit a dependence on geometry which is similar to that for ^1H and ^{13}C . For the particular case of ^1H - ^{15}N interactions, a Karplus type relationship between $^3J_{\text{NH}}$ and dihedral angle exists,⁴⁸ however the range of values for the couplings is small, the maximum values being *ca* 8 Hz. An added complication here is the suggestion of a sign reversal for dihedral angles in the range of 80 – 90° , thus rendering detailed data comparisons difficult and indeed dangerous for structurally unrelated molecules.

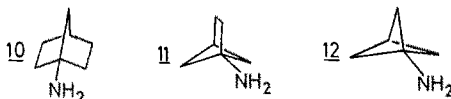
One test of the validity of vicinal ^1H - ^{15}N couplings for conformational analysis has been reported⁴⁹ for the amino acid leucine (below). In this case, the rotamer populations derived from the $^3J_{\text{NH}}$ data are in reasonable accord with results based on $^3J_{\text{HH}}$ and $^3J_{\text{CH}}$ coupling constants.



Rather few studies of vicinal ^{13}C - ^{15}N couplings have been reported. Available data indicate that the magnitudes of these couplings are small and hence detailed correlations with geometry are difficult. Typical data are available for aromatic oximes⁵⁰ in which the ^{15}N -C-C- ^{13}C angle is altered due to the influence of the *ortho* methyl groups. For the mesityl derivative below, X-ray results⁵¹ indicate that the oxime function is rotated substantially (*ca* 70°) out of the plane of the aromatic ring. In this case $^3J_{\text{NC}}$ is 1.2 Hz. For the related molecule which lacks the *ortho* methyl groups and is presumably nearly planar, the $^3J_{\text{NC}}$ is 2.9 Hz.

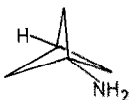


Recently⁵² a series of ^{15}N labelled 1-aminobicyclanes have been synthesized and the couplings to ^{15}N examined. For the series **10**, **11** and **12** (below) the $^3J_{\text{NC}}$ values to the bridgehead carbons are 1.99, 4.03 and 5.57 Hz respectively. The ratio of these couplings corresponds to that expected on the basis of the number of vicinal coupling pathways available, there being one in **10**, two in **11** and three in **12**.



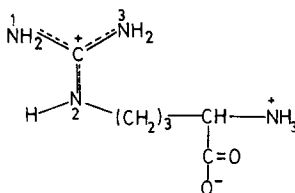
INDO MO calculations have been carried out on these molecules and the results suggest that in highly strained systems, there is a substantial contribution to $^3J_{\text{NC}}$ arising from through-space interactions and these oppose through-bond effects.

A further point of interest in these results is the remarkably large (6.11 Hz) long range (4-bond) coupling between the ^{15}N and the proton on the unsubstituted bridgehead carbon of **12**. The existence of three 4J "W" coupling pathways is no doubt a major factor in this observation.



4.6. Stereochemical dynamics studied by ^{15}N NMR

^{15}N NMR has proven to be useful for studying dynamic processes such as rates of NH proton exchange in molecules that are not amenable to ^1H NMR examination.^{53,54} Also it has been utilized to determine barriers to isomerization about the C-N2 bond of L-arginine (below). In this molecule, restricted rotation about the C-N2 bond will render the N1 and N3 protons non-equivalent. ^1H NMR cannot, however, be applied to this problem due to the existence of temperature dependent quadrupole broadening between ^{14}N and its bonded hydrogens.



In the ^{15}N NMR spectrum⁵⁵ at 25°C , the resonances for N1 and N3 appear as a singlet due to rapid rotation about the C-N2 bond on the NMR timescale. Below 4°C , separate ^{15}N resonances are observed with limiting chemical shift difference of 2.4 ppm. Detailed lineshape analysis yields the following activation parameters for isomerization in the guanidinium group of arginine at pH 7.0: $\Delta G^\ddagger = 12.1$ kcal/mol, $\Delta H^\ddagger = 21.7$ kcal/mol and $\Delta S^\ddagger = 36$ e.u.

4.7. Molecular dynamics as studied by ^{15}N T_1 s and ^1H - ^{15}N nOes

The spin-lattice relaxation time, T_1 , of a ^{15}N nucleus can be a sensitive probe of its correlation time, τ_c , which is in turn a measure of the rotational freedom of the molecular segment. For protonated nitrogens, the dipole-dipole relaxation mechanism usually dominates over the other three possible relaxation pathways.¹ In mobile liquids where the motional narrowing condition as depicted in Fig. 2 applies, measurement of the ^1H - ^{15}N nOe permits the evaluation of the contribution of the dipole-dipole mechanism to the overall spin-lattice relaxation.¹ For dominating dipole-dipole relaxation, $1/T_1 \propto \tau_c$.

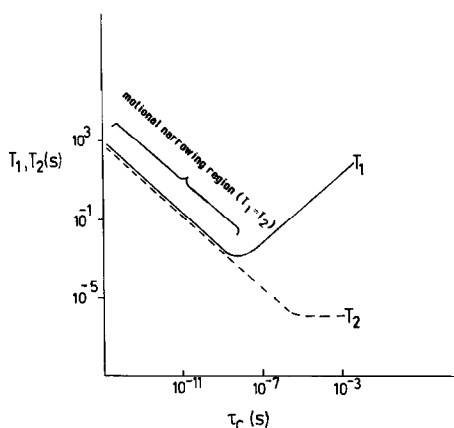


Fig. 2. Correlation time dependence of T_1 (for dominant dipole-dipole relaxation) and T_2 , at ^{15}N resonance frequency of 20 MHz.

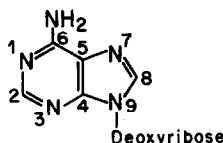
To a first approximation, τ_c can be expressed as shown in Eq. (2) below,

$$\tau_c = \frac{4\pi\eta a^3}{3kT} \quad (2)$$

where η is the viscosity of the solution, a is the radius of the molecule, T is the absolute temperature and k is the Boltzmann constant.

The relationship between ^{15}N T_1 s and molecular mobility has been used in the case of the three ^{15}N enriched amino acids alanine, arginine and glutamine to probe their intracellular environment in intact *Neurospora crassa* mycelia.⁵⁶ Association of these amino acids with other cellular components increases the effective molecular sizes and hence increases the correlation time. This results in shortened ^{15}N T_1 s for the amino acids in the cytoplasm relative to those observed in the culture medium.

More recently⁵⁷ ^{15}N T_1 s have been used along with the temperature dependence of ^{15}N chemical shifts, to monitor oligonucleotide helix to coil transitions. Specifically $d[\text{CGTACG}]$ has been examined using ^{15}N enriched deoxyadenosine (below) at the N6 and N1 sites.



The N6 position, with two directly bonded nitrogens was shown to undergo efficient dipole-dipole relaxation. For the nonprotonated N1 site, relaxation mechanisms other than dipole-dipole may be operative. The temperature dependence of the ^{15}N T_1 for N1, however indicates that spin-rotation relaxation is not a major contributor. Since the other two mechanisms are unlikely in this instance it appears that N1 also relaxes primarily via a dipole-dipole pathway.

The ^{15}N T_1 for N1 enriched deoxyadenosine shows a linear temperature dependence. By contrast, in the hexamer, there is a marked change in slope of the T_1 vs temperature plot. There is a general decrease in T_1 with decreasing temperature which indicates that the hexamer is still on the motional narrowing part of the T_1 vs τ_c plot (Fig. 2). The most interesting point however is that, as the temperature is lowered, there is a pronounced slope change indicating a further decrease in T_1 and hence a reduction in mobility. The temperature at which the change in slope occurs coincides with that known from other methods for the transition from the coil to the more organized, i.e. less mobile helical form.

Dynamic structural information about double-stranded DNA has been obtained from a study of the ^1H - ^{15}N nOe.⁵⁸ ^{15}N enriched DNA was isolated from *E. coli* cells grown on a medium containing ^{15}N enriched ammonium chloride. Assuming a dominance of dipole-dipole relaxation for proton-bearing nitrogens, the theoretical dependence of the nOe on the lifetimes of rotamers about the N-deoxyribose bond has been calculated for a 30.4 MHz ^{15}N observation frequency. On the basis of the results of these calculations, negative ^{15}N resonances observed are attributed to protonated nitrogens on single stranded DNA, while the deshielded positive resonances are attributed to protonated nitrogens on double-stranded DNA.

5. METAL BINDING PHENOMENA

In most cases of interactions of metal ions with organic ligands, the protons and carbons of the ligands do not become directly bonded to the metal through complex formation. Consequently the

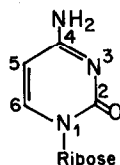
^1H and ^{13}C NMR parameter changes reflect essentially second order effects. Accordingly there is a special interest in the study of metal ion binding to nitrogen containing ligands via ^{15}N NMR spectroscopy of the nitrogens which are directly involved in the binding to the metal.

5.1. Metal ion binding to nucleic acid components

The biological and medical importance of metal ion interactions with nucleotide components is now well recognized. In the particular case of platinum complexes there has been widespread interest since the discovery⁵⁹ of the antitumor activity of *cis*-[Pt(NH₃)₂Cl₂], “*cis*-platinum”. The mode of action of “*cis*-platinum” appears to be via complexation of the metal with one or more nitrogens of the nucleotide bases of DNA.⁶⁰

In order to delineate more specifically the nature of these binding interactions, a study of the ^{15}N NMR behaviour of the complexes of *cis*-platinum with five nucleosides was carried out.⁶¹ For thymidine and uridine, no appreciable amounts of platinum complexes were obtained in aqueous solution after a reaction time of two weeks at room temperature. In the case of adenosine, a mixture of several mono and bis adducts was obtained which precluded a meaningful analysis of the ^{15}N spectra. Unambiguous results were obtained, however, for the cytidine and guanosine cases.

For cytidine, below, a bis complex is formed in which the ^{15}N shifts of the coordinated ligand are presented in Table 4.



Comparison of these values with those for the uncomplexed nucleoside indicate that the N1 resonance is unaffected, while N3 shifts upfield by 82 ppm in the complex and the NH₂ moves downfield by 10 ppm. The large upfield shift of N3 in the complex indicates that this is the preferred platination site, with the shifts being of the same magnitude and direction as those that occur upon protonation. For the bis guanosine complex i.e. *cis*-[Pt(NH₃)₂(Guo)₂]²⁺, the ^{15}N resonance for N7 is shifted upfield by 103.7 ppm relative to the uncomplexed nucleoside (Table 4) while the other four nitrogens are relatively unaffected. This can be taken as evidence for specific N7 platination.

It is to be noted that the ^{15}N shifts of ammonia molecules complexed to platinum appear 40–70 ppm upfield of that for free ammonia. This is opposite to the direction of the protonation shifts of primary amines.¹

For methylated nucleosides which are important in the study of mutagenesis, a symmetrical bidentate complex has been obtained from the reaction of 1-methylguanosine with *cis*-platinum.⁶² From ^{15}N NMR it is clear that the N7 site is the only nitrogen which is affected appreciably by platination. Its resonance is shifted upfield by nearly 100 ppm relative to 1-methylguanosine itself.

Table 4. ^{15}N chemical shifts (δ_{N} from NH₃ ± 0.1). For cytidine (C) and guanosine (G) and their bis complexes with *cis*-[Pt(NH₃)₂Cl₂]⁶¹

Compound	N-1	N-3	N-7	N-9	NH ₂
C	152.1	206.7			93.0
<i>cis</i> -[Pt(NH ₃) ₂ C ₂] ²⁺	152.2	124.8			103.4
G	146.2	164.8	246.0	169.0	72.3
<i>cis</i> -[Pt(NH ₃) ₂ G ₂] ²⁺	147.7	164.5	142.3	173.1	75.5

The influence of Hg^{+2} , Zn^{+2} and Ba^{+2} complexation on the ^{15}N chemical shifts of adenosine, cytidine and guanosine in DMSO solution has been studied.⁶³ According to the Lewis acid strength classification, the Hg^{+2} ion is deemed to be relatively "soft", the Zn^{+2} ion intermediate and the Ba^{+2} ion is relatively "hard". For all three nucleosides, Ba^{+2} complexation caused no measurable change in the ^{15}N shifts, presumably due to the preference of Ba^{+2} for oxygenated rather than nitrogenated binding sites.

For adenosine (below) addition of 1 equivalent of HgCl_2 induces the chemical shift changes depicted in Fig. 3.



The N1 resonance is most affected and experiences an upfield shift of 9.5 ppm suggesting that it is the preferred site of mercuration. This upfield shift at N1 is in the same direction as that found earlier for protonation.²⁰ The minor upfield shift for N7 suggests that N1 may not be the exclusive complexation site. The minor downfield shifts of the remaining three nitrogens are probably due to their involvement in conjugation with one of the metallated nitrogens.

It is of interest to note that addition of Zn^{+2} to adenosine reverses the trends found for N1 and N7 upon mercuration. These data suggest that there are different mixes of N1 and N7 metallated complexes present in these two cases. Such a conclusion is in agreement with previous studies⁶⁴ which utilized ^1H and ^{13}C NMR as well as Raman difference spectra. The ^{15}N method has the advantage, however, that relative nitrogen site selectivities can be obtained.

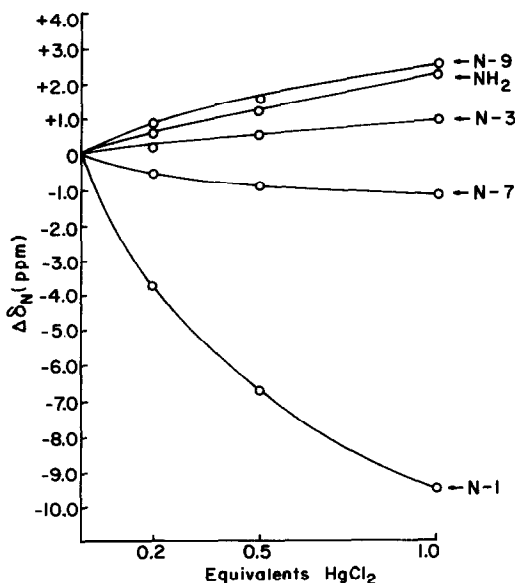
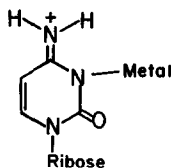


Fig. 3. Adenosine ^{15}N chemical shift changes induced by successive additions of HgCl_2 .

For cytidine, the effects of Hg^{+2} and Zn^{+2} addition on the ^{15}N chemical shifts are very similar in direction to those found for platination.⁶⁰ The upfield shift at N3 is attributed to direct metallation while the downfield shift at the NH_2 group presumably arises from the contribution of the NH_2 function in the resonance form depicted below.



For guanosine and the structurally related inosine system²¹ the ^{15}N results indicate that both Hg^{+2} and Zn^{+2} bind preferentially at N7.

The interaction of the environmentally important methylmercury(II) ion with some mononucleotides has also been examined recently by ^{15}N NMR.⁶⁵ Many organomercurials including this system are known to cause chromosomal damage⁶⁶⁻⁶⁸ probably owing to the direct interaction of the organomercurial with nucleic acid components.

For 3'-CMP, addition of CH_3HgOH induces a substantial upfield shift at N3 and minor deshielding effect at the NH_2 and N1 sites. Accordingly a preference for the N3 binding site is indicated. The nearly equal downfield shifts for the NH_2 and N1 resonances are consistent with these sites being conjugated with the methylmercurated nitrogen.

In the case of 5'-GMP, addition of 1 equivalent of CH_3HgOH at pH 8.0 induces a *downfield* shift of 49.9 ppm in the N1 resonance whereas the resonances for the other four nitrogens are affected by less than 3 ppm. From UV difference spectra⁶⁹ on guanosine, it appears that N1 is the preferred binding site for methylmercury at pH 8.0, although no work on the related 5'-GMP has been published. The explanation for the apparently anomalous downfield shift of N1 upon mercuration comes from the fact that N1 appears to deprotonate before it methylmercurates. It is known for several guanosine monophosphates, that deprotonation occurs at pH 8.0 leading to a downfield shift of 60 ppm for N1 upon full deprotonation.²² Thus the observed deshielding of *ca* 50 ppm at N1 is probably due to a "normal" upfield shift of *ca* 10 ppm arising from methylmercuration superimposed on the known deshielding effect of 60 ppm for deprotonation. The usual N7 binding site in the guanine residue of 5'-GMP methylmercurates below pH 6.0.

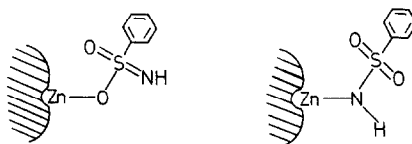
On the theoretical side, the observed "normal" trend of upfield ^{15}N shifts for pyridine type nitrogens upon protonation and metallation can be rationalized in terms of dominant contributions from the second order paramagnetic effect. The paramagnetic shielding term (Eq. 1) contains the average electronic excitation term ΔE , which corresponds in a general way to the $n-\pi^*$ transition energy. Complexation of a positively charged metal ion or a proton with the nitrogen lone pair would be expected to lead to an increase in the $n-\pi^*$ transition energy. As a result, a decreased contribution from the paramagnetic term will result and hence an upfield shift in the ^{15}N resonance.

5.2. Metal-nitrogen binding in amino acid complexes and enzymes

The interaction of cobalt(III) with a number of amino acids has been examined via ^{15}N NMR chemical shifts.⁷⁰ For a series of complexes of the type λ -*cis*-(NO_2)-*trans*-(NH_2)- $[\text{Co}(\text{NO}_2)_2(\text{Am})_2]^{(+/-)}$, where AmH represents the amino acid, upfield shifts of 24-42 ppm were observed on replacement of an amino proton by cobalt(III). In very symmetrical complexes such as $[\text{Co}(\text{NH}_3)_5(^{15}\text{NH}_3)]\text{Cl}_3$ the ^{15}N signal of nitrogen bonded to ^{59}Co is observed to be split into an octet due to spin coupling to the $I = 7/2$ ^{59}Co nucleus.⁷¹ In less symmetrical structures however, fast quadrupolar relaxation effectively prevents this coupling from being resolved.

More recently⁷² a series of complexes of the type $[\text{Co}(\text{ox})_x(\text{gly})_y(\text{en})_z]$, where $\text{oxH}_2 = \text{oxalic acid}$, $\text{glyH} = \text{glycine}$ and $\text{en} = \text{ethylenediamine}$ have been examined. Upfield ^{15}N shifts of 19–62 ppm are found upon complexation with cobalt. In addition there are strong stereochemical shift dependencies; for example a nitrogen of an amino group *trans* to oxygen is shielded by *ca* 18 ppm more than a corresponding group *trans* to nitrogen.

A number of studies have appeared in which ^{15}N NMR has been utilized to examine the binding of inhibitors to the zinc metalloenzyme carbonic anhydrase.^{73–75} In the case of a cyanate inhibitor⁷³ the cyanate ^{15}N resonance moved 34 ppm upfield upon binding to the human enzyme. Comparison of this result with those for model complexes indicates that a Zn–N bond is formed in the complex. For the benzenesulfonamide inhibitor,⁷³ an upfield ^{15}N shift of 17 ppm was found for the bound *vs* the free sulfonamide anion, again suggesting Zn–N coordination. The Zn–O and Zn–N binding modes for this enzyme are depicted below.



For N-(2-aminophenyl)benzenesulfonamide, the Zn–O mode is deemed to be operative. In this case, the sulfonamide nitrogen experiences a *deshielding* of 1.2 ppm on coordination of zinc to the anionic ligand. Thus it appears that ^{15}N NMR can be used to distinguish the oxygen *vs* nitrogen binding modes with the metalloenzyme.

In the case of ^{111}Cd -substituted bovine carbonic anhydrase,⁷⁴ the binding of the inhibitor 4-fluoro-N-hydroxybenzenesulfon[^{15}N]amide was probed via ^{15}N methods. The observation of an 8 Hz coupling between ^{15}N and ^{111}Cd was indicative of binding of the enzyme to the inhibitor via a nitrogen rather than an oxygen atom.

Recently⁷⁵ the binding of human carbonic anhydrase with the carbonyl hydration substrate pyruvamide has been studied. Employing ^{15}N enriched substrate and ^1H coupled ^{15}N spectra, the binding of the deprotonated amide anion form of pyruvamide to the Zn of the enzyme was demonstrated.

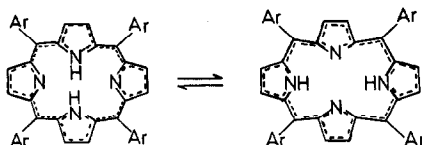
6. ^{15}N NMR STUDIES OF SOLIDS

Techniques have now been developed so that high resolution NMR spectra of solids can be obtained on a routine basis. For relatively low abundance nuclei such as ^{13}C and ^{15}N , the cross-polarization (CP) technique⁷ can be used to advantage to increase detection sensitivity. Dipolar interactions present in solids can be effectively averaged to zero by magic angle spinning (MAS).⁷⁵ Rapid sample spinning is employed to minimize the effects of chemical shift anisotropy. These procedures, combined with high power ^1H decoupling allow one to obtain high quality ^{13}C and ^{15}N CPMAS spectra on solids in time periods comparable to those for NMR in solution. The chemical applications and underlying principles of solid state NMR have been reviewed recently.⁷⁷

6.1. Proton transfer kinetics via solid phase ^{15}N NMR

There is considerable interest in studying proton transfer reactions in solids by dynamic NMR methods. In some cases rate constants may be obtained at low temperatures in solids which are not accessible in solution.⁷⁸ A possible complication in the interpretation of the solid phase kinetic data arises if there is a kinetic solid state effect (KSSE)—i.e. if proton transfer rate constants in solution and in the solid are markedly different at the same temperature. Indeed for tropolone, the KSSE is so large that proton transfer is not observable in the solid state on the NMR timescale.⁷⁹

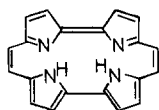
In the case of ^{15}N -enriched free-base *meso*-tetraarylporphines, solid phase ^{15}N NMR has been employed to study a tautomerism which occurs in both solution and in the solid state.⁸⁰ For the tetra-*p*-tolyl derivative (below), two ^{15}N resonances are observed in the solid at low temperature



which indicates that the proton migration depicted above is slow on the NMR timescale. At higher temperature the lines broaden and coalesce and the derived kinetic data are very similar to those found in solution for *meso*-tetraphenylporphine itself.

For triclinic tetraphenylporphine, the ^{15}N CPMAS spectra indicate rapid proton migration in the solid between two very unequally populated tautomers. Such information cannot be obtained from X-ray analysis, thereby illustrating the utility of the solid phase NMR experiment.

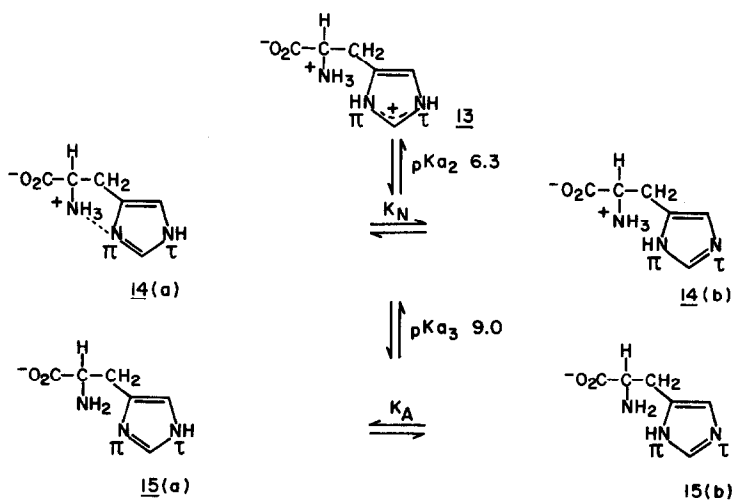
In crystalline porphine itself, ^{15}N CPMAS NMR has been employed recently for measurement of NH tautomerism rates and activation parameters.⁸¹ By contrast, in solid porphycene (below) the



rates of tautomerization, even at low temperatures, are too fast to be examined via ^{15}N NMR.

6.2. ^{15}N CPMAS studies of proteins and other biopolymers

The first study via ^{15}N of an unsaturated nitrogenous base-conjugate acid pair in the solid state was carried out on L-histidine⁸² (below), which had been ^{15}N enriched in the imidazole ring.



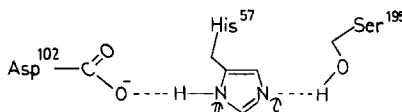
For imidazole itself, the ^{15}N MAS spectrum in the solid exhibits two resonances separated by 72 ppm, indicating that tautomeric exchange is slow in the solid on the NMR timescale. The average of the two chemical shifts in the solid is the same as that for the single ^{15}N observed in solution.

In the case of histidine, five distinct species must be considered in order to interpret the solution and solid phase ^{15}N data.

In solutions at low pH, only **13** is present. As the pH is increased the imidazole ring deprotonates first and the forms **14(a)** and **14(b)** increase progressively relative to **13**. Since these three forms are in rapid exchange, the ^{15}N spectrum shows averaged chemical shifts. At pH 8.0 the imidazole ring completely deprotonates and both nitrogens are deshielded relative to the cationic species. The signal for the π nitrogen is *ca* 50 ppm more deshielded than that of the τ nitrogen indicating that form **14(a)** predominates over **14(b)**. At high pH, the NH_3^+ group deprotonates thereby eliminating the hydrogen bonding interaction present in **14(a)**. This leads to a redistribution of tautomers in **15** so that **15(a)** is not as highly favoured over **15(b)** as was the case in **14(a)** vs **14(b)**.

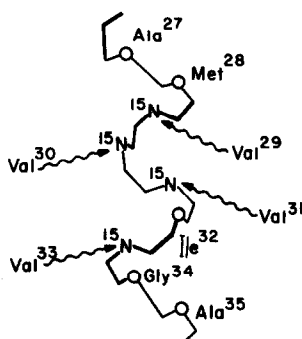
Several solid samples of histidine which had been prepared from solutions with pH values from 2.0–12.5 were examined.⁸² In the solid, exchange between cationic and neutral forms is slow so that separate resonances are observed for each species. Interestingly, form **14(a)** appears to be even more highly favoured in the solid than in solution, due to persistent hydrogen bond formation as indicated above. At pH 9.5 and higher, a minor downfield shift is observed for the π nitrogen but no change is noted for the τ position. Thus it appears in the solid that the $\text{N}^{\tau}\text{-H}$ tautomer is highly favoured even in the absence of the hydrogen bond.

In related work,⁸³ histidine enriched in ^{15}N at the imidazole nitrogens has been incorporated into the catalytic triad of the enzyme α -lytic protease. High resolution solid state ^{15}N spectra of lyophilized enzyme powders prepared from solutions with pH values from 4.9 to 9.3 were obtained. The behaviour of the ^{15}N resonances as a function of “pH” in the solid is similar to that found in solution with the exception of the His-57 residue. In this residue the proton exchange is fast on the NMR timescale in solution, but slow in the solid. The ^{15}N MAS chemical shifts in the solid demonstrate that the $\text{N}^{\tau}\text{-H}$ tautomer (below) predominates in powders prepared at high pH. In addition, $\text{N}^{\tau}(\text{H})$ is shown to participate in a strong hydrogen bond in powders prepared at both high and low pH.



Solid phase ^{15}N NMR has also been employed to study the nature of the Schiff base present in bacteriorhodopsin.⁸⁴ This material is the single protein of the purple membrane of *Halobacterium halobium* and possesses, as its chromophore, the polyene aldehyde retinal which is Schiff base linked to the ϵ -amino group of a lysine sidechain. In dark adapted ^{15}N -enriched bacteriorhodopsin, an upfield shift of 150 ppm was found relative to material which had undergone the photocycle. This result is taken as strong evidence for the existence of protonated rather than unprotonated Schiff base in lyophilized dark adapted purple membrane.

Spatial proximity between nitrogens can be probed via ^{15}N - ^{15}N spin exchange experiments in the solid phase. If ^{15}N enriched material is studied, off-diagonal cross peaks will be observed in the ^{15}N - ^{15}N COSY experiment if the ^{15}N sites are close in space. The method has been employed to study solid state structure of viral coat protein.⁸⁵ In this material, which was synthesized with only four ^{15}N labelled sites, there are four spatially proximate valine sites as depicted in the α -helical backbone conformation below. Chemical shift resolution among these chemically similar sites occurs because of alignment of these molecules in a particular orientation with respect to the magnetic field.



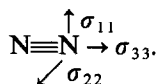
The valine-30 residue is only about 2.8 Å from valine-29 or valine-31. Accordingly, cross peaks are expected and indeed found between the val-30 ^{15}N resonance and those for val-29 and val-31. By contrast, the nitrogens of val-29 and val-33 are more than 6 Å apart and do not give rise to a cross peak. One can effectively rule out spin exchange between the backbones of neighbouring protein subunits because their distance of closest approach is *ca* 8 Å. In the spectrum of the uniformly ^{15}N labelled virus, the spin exchange experiment was employed for specific ^{15}N resonance assignment.

The complementary nature of solution and solid phase ^{15}N spectra for studying backbone dynamics has been demonstrated recently for the same viral coat protein.⁸⁶ Motions which occur with frequencies near the Larmor frequencies of *ca* 10^9 Hz in solution can be studied by techniques such as the ^1H - ^{15}N nOe⁵⁸ which are dependent on the T_1 relaxation mechanism. In solids, the powder pattern lineshapes are averaged by motions which occur rapidly relative to the frequency width of the powder pattern. The ^{15}N powder pattern width arises from chemical shift anisotropy and normally covers a range of *ca* 10^4 Hz. Thus the solution and solid phase techniques complement each other since they are sensitive to motions on markedly different timescales.

The calculated solid state phase ^{15}N spectra showing the effects of motional averaging for the amide functional group have been published.⁸⁶ These calculated spectra have been used as a basis for interpretation of experimental results. In the instance of uniformly ^{15}N labelled viral coat protein, the experimental spectra are interpreted in terms of at least ten mobile sites on the 10^4 Hz timescale and only seven mobile sites on the 10^9 Hz timescale.

6.3. ^{15}N Chemical shift tensors

In solution or in MAS spectra of solids, the observed isotropic chemical shift represents the result of motional averaging of the chemical shift tensors σ_{11} , σ_{22} and σ_{33} as depicted below for the case of N_2



If single crystals are available, one can measure the individual shift tensors by determination of the chemical shifts as a function of the orientation of the crystal in the magnetic field.⁷⁷ These tensors are often large and disparate and may have opposite substituent effects or even opposite signs. Any successful ^{15}N chemical shift theory will have to deal with each of the separate tensor parameters for a given functionality.

Data on ^{15}N chemical shift tensors are also important experimentally for studies of both solutions and solids. For solutions, sensitivity considerations dictate that the highest possible magnetic fields should be employed. At high field, however, the chemical shift anisotropy (CSA) relaxation mechanism¹ may become dominant and produce spectral line broadening. Such an effect will be particularly important in biopolymers,⁸⁷ so that a balance between sensitivity and resolution may have to be struck for any given problem.

In solid state spectra, line broadening can be useful for studying molecular motion (*vide supra*) if one has knowledge of the appropriate chemical shift tensors. Also from a practical point of view, knowledge of the size of chemical shift tensors is valuable for determining the optimal spinning rate in the MAS experiments and for the assignment of centrebands and sidebands in such spectra, since the number of sidebands n is related to the shift tensor $\Delta\sigma$ (in Hz), and the spinning rate r (in Hz) by Eq. 3 (below)

$$n \sim [(\Delta\sigma/r) - 1]. \quad (3)$$

A further interesting possibility arises in solids if the tensors are known and that is the study of the anisotropy of exchange processes.⁸⁸

To date the available data on ^{15}N chemical shift tensors reflect the hybridization and symmetry about the nitrogen in each case. For sp^3 hybridized nitrogen, the shift anisotropies have been found^{87,89} to be relatively small (*ca* 20 ppm). By contrast, the less symmetrical sp^2 hybridized nitrogens display anisotropic chemical shift tensors of 600–800 ppm.⁹⁰ In the peptide linkage which has only partial double bond character, the anisotropic chemical shift tensor is *ca* 150 ppm in the case of glycyl–glycine.⁹¹ Such data should be valuable in the interpretation of solid state ^{15}N NMR of peptides and proteins since the magnitude and orientation of this tensor are expected to be characteristic of this functional group with only minor variations due to differing amino acid sidechains.

6.4. Measurement of ^{15}N -H bond distances via solid state ^{15}N NMR

Recently, experimental conditions have been reported for carrying out high resolution two dimensional dipolar–chemical shift experiments in the solid state.⁹² Such measurements permit the location of protons in polycrystalline or amorphous solids, with bond distances precise to within 0.005 Å. The only other source of such data is single crystal electron diffraction, so that the NMR method provides the only probe if suitable single crystals are not available. The peptide linkages in a number of ^{15}N labelled substrates have been examined. In general the ^{15}N -H distances obtained via this method are consistently *ca* 0.035 Å longer than those obtained via single crystal neutron diffraction. It is suggested that this difference arises from vibrational averaging of the dipolar ^{15}N - ^1H interaction. Although the method is illustrated only for ^{15}N - ^1H , it should also be applicable to the determination of distances between other spin pairs such as ^1H - ^{13}C , ^1H - ^{31}P and ^{13}C - ^{15}N .

6.5. Characterization of surface bound species via ^{15}N NMR in solids

The adsorption of pyridine on γ -alumina has been examined via both solid state ^{13}C ⁹³ and ^{15}N ⁹⁴ methods. The ^{13}C results were used to identify only a single type of adsorbed species, whereas four distinct species could be identified via ^{15}N CPMAS methods, thereby demonstrating the superiority of the latter method for this type of study. The ^{15}N chemical shifts are very sensitive to the nature of the bound species, as exemplified by the following results: physically sorbed pyridine, $\delta_{\text{N}} = 312$; physically sorbed and hydrated pyridine, $\delta_{\text{N}} = 298$; Lewis acid site I sorbed pyridine, $\delta_{\text{N}} = 266$ and Lewis acid type II sorbed pyridine, $\delta_{\text{N}} = 238$. In addition a pyridinium ion species was identified with $\delta_{\text{N}} = 202$ which may be due to the presence of pyridinium carbonate or bicarbonate in samples which had been exposed to air for several hours.

In subsequent work⁹⁵ the Lewis acid binding sites have been further characterized. The resonance at $\delta_{\text{N}} = 238$ has been assigned to pyridine which occupies the site formed by octahedrally coordinated Al^{+3} cations, whereas the resonance at $\delta_{\text{N}} = 266$ arises from pyridine which occupies the site formed by tetrahedrally coordinated Al^{+3} cations. The relative distributions of the tetrahedral and octahedral Lewis acid sites have been determined as a function of surface preparation conditions.

Acknowledgements—I wish to thank Professor J. D. Roberts for his comments on the manuscript and Professors R. G. Griffin and E. W. Randall for provision of preprints. Financial support for the work described from the author's laboratory has been provided by the Natural Sciences and Engineering Research Council of Canada.

REFERENCES

- ¹ G. C. Levy and R. L. Lichter, *^{15}N Nuclear Magnetic Resonance Spectroscopy*. Wiley, New York (1979).
- ² G. J. Martin, M. L. Martin and J. Gouesnard, *^{15}N NMR Spectroscopy*. Springer, Berlin (1981).
- ³ M. Witanowski, L. Stefaniak and G. A. Webb, *Annual Reports on NMR Spectroscopy*, Vol. 11B (Edited by G. A. Webb), Academic Press, New York (1981).
- ⁴ W. von Philipsborn and R. Muller, *Angew. Chemie. Inter. Ed.* **25**, 383 (1986).
- ⁵ J. H. Noggle and R. E. Schirmer, *The Nuclear Overhauser Effect—Chemical Applications*. Academic Press, New York (1972).
- ⁶ G. C. Hawkes, W. M. Litchman and E. W. Randall, *J. Mag. Res.* **19**, 255 (1975).
- ⁷ G. A. Morris, *J. Am. Chem. Soc.* **102**, 428 (1980).
- ⁸ A. Bax, C.-N. Niu and D. Live, *J. Am. Chem. Soc.* **106**, 1150 (1984).
- ⁹ D. H. Live, D. G. Davis, W. C. Agosta and D. Cowburn, *J. Am. Chem. Soc.* **106**, 6104 (1984).
- ¹⁰ L. Muller, *J. Am. Chem. Soc.* **101**, 4481 (1979).
- ¹¹ V. Sklenar and A. Bax, *J. Mag. Res.* **71**, 379 (1987).
- ¹² J. A. Pople, W. G. Schneider and H. J. Bernstein, *High Resolution Nuclear Magnetic Resonance*. McGraw-Hill, New York (1959).
- ¹³ M. Witanowski, L. Stefaniak and H. Januzewski, in *Nitrogen NMR* (Edited by M. Witanowski and G. A. Webb), Plenum Press, New York (1973).
- ¹⁴ R. L. Lichter and J. D. Roberts, *J. Am. Chem. Soc.* **94**, 2495 (1972).
- ¹⁵ R. O. Duthaler and J. D. Roberts, *J. Am. Chem. Soc.* **100**, 3889 (1978).
- ¹⁶ J. P. Warren and J. D. Roberts, *J. Phys. Chem.* **78**, 2507 (1974).
- ¹⁷ J. B. Stothers, *Carbon-13 NMR Spectroscopy*. Academic Press, New York (1972).
- ¹⁸ G. C. Levy and G. L. Nelson, *Carbon-13 Nuclear Magnetic Resonance for Organic Chemists*. Wiley Interscience, New York (1972).
- ¹⁹ P. B. Dervan, M. E. Squillacote, P. M. Lahti, A. P. Sylwester and J. D. Roberts, *J. Am. Chem. Soc.* **103**, 1120 (1981).
- ²⁰ V. Markowski, G. R. Sullivan and J. D. Roberts, *J. Am. Chem. Soc.* **99**, 714 (1977).
- ²¹ G. W. Buchanan and M. J. Bell, *Can. J. Chem.* **61**, 2445 (1983).
- ²² P. Buchner, W. Maurer and H. J. Ruterjans, *J. Mag. Res.* **29**, 45 (1978).
- ²³ N. C. Gonnella, H. Nakanishi, J. B. Holtwick, D. S. Horowitz, K. Kanamori, N. J. Leonard and J. D. Roberts, *J. Am. Chem. Soc.* **105**, 2050 (1983).
- ²⁴ S. J. Benkovic, D. Sammons, W. L. F. Amarego, P. Waring and R. Inners, *J. Am. Chem. Soc.* **107**, 3706 (1965).
- ²⁵ J. M. Schulman and T. Venanzi, *J. Am. Chem. Soc.* **98**, 4701 (1976).
- ²⁶ G. A. Gray, G. W. Buchanan and F. G. Morin, *J. Org. Chem.* **44**, 1768 (1979).
- ²⁷ G. A. Gray and T. A. Albright, *J. Am. Chem. Soc.* **98**, 3857 (1976).
- ²⁸ G. W. Buchanan and V. L. Webb, *Tetrahedron Lett.* **24**, 4519 (1983).
- ²⁹ R. O. Duthaler, K. L. Williamson, D. P. Giannini, W. H. Bearden and J. D. Roberts, *J. Am. Chem. Soc.* **99**, 8406 (1977).
- ³⁰ N. K. Wilson and J. B. Stothers, *Topics in Stereochem.* **8**, 1 (1973).
- ³¹ R. L. Lichter and J. D. Roberts, *Org. Mag. Res.* **6**, 636 (1974).
- ³² G. W. Buchanan, F. G. Morin and R. R. Fraser, *Can. J. Chem.* **58**, 2442 (1980).
- ³³ M. P. Sibi and R. L. Lichter, *J. Org. Chem.* **42**, 2999 (1977).
- ³⁴ W. H. Pirkle, S. D. Beare and T. G. Burlingame, *J. Org. Chem.* **34**, 470 (1969).
- ³⁵ W. H. Pirkle, D. L. Sikkenga and M. S. Pavin, *J. Org. Chem.* **42**, 384 (1977).
- ³⁶ R. Dyllick-Brenzinger and J. D. Roberts, *J. Am. Chem. Soc.* **102**, 1166 (1979).
- ³⁷ J. A. Sogn, W. A. Gibbons and E. W. Randall, *Biochemistry* **12**, 2100 (1973).
- ³⁸ G. E. Hawkes, E. W. Randall and C. H. Bradley, *Nature* **257**, 767 (1975).
- ³⁹ K. L. Williamson, L. G. Pease and J. D. Roberts, *J. Am. Chem. Soc.* **101**, 714 (1979).
- ⁴⁰ H. Kessler, W. Hehlein and R. Schuck, *J. Am. Chem. Soc.* **104**, 4534 (1982).
- ⁴¹ V. F. Bystrov, *Prog. Nuc. Mag. Res. Spect.* **10**, 41 (1976).
- ⁴² G. E. Hawkes, L. Y. Liam and E. W. Randall, *J. Mag. Res.* **56**, 539 (1984).

- ⁴³ G. E. Hawkes, L. Y. Liam, E. W. Randall, K. D. Sales and E. H. Curzon, *Eur. J. Biochem.* **166**, 437 (1987).
- ⁴⁴ A. S. Arseniev, G. Wider, F. J. Joubert and K. Wuthrich, *J. Mol. Biol.* **159**, 323 (1982).
- ⁴⁵ D. Crépeaux and J. M. Lehn, *Mol. Phys.* **14**, 547 (1968).
- ⁴⁶ G. W. Buchanan and B. A. Dawson, *Can. J. Chem.* **55**, 1437 (1977).
- ⁴⁷ G. W. Buchanan and B. A. Dawson, *Org. Mag. Res.* **13**, 293 (1980).
- ⁴⁸ V. F. Bystrov, Y. D. Garilov and V. N. Solcan, *J. Mag. Res.* **19**, 123 (1975).
- ⁴⁹ A. J. Fischman, H. R. Wyssbrod, W. C. Agosta and D. Cowburn, *J. Am. Chem. Soc.* **100**, 54 (1978).
- ⁵⁰ G. W. Buchanan and B. A. Dawson, *Can. J. Chem.* **56**, 2200 (1978).
- ⁵¹ S. Fortier, G. I. Birnbaum, G. W. Buchanan and B. A. Dawson, *Can. J. Chem.* **58**, 191 (1980).
- ⁵² E. W. Della, B. Kasum and K. P. Kirkbride, *J. Am. Chem. Soc.* **109**, 2746 (1987).
- ⁵³ M. Nee, C. Yu, M. E. Squillacote and J. D. Roberts, *Org. Mag. Res.* **18**, 125 (1982).
- ⁵⁴ C. Yu, I. Yavari and J. D. Roberts, *Org. Mag. Res.* **18**, 74 (1982).
- ⁵⁵ K. Kanamori and J. D. Roberts, *J. Am. Chem. Soc.* **105**, 4698 (1983).
- ⁵⁶ K. Kanamori, T. L. Legerton, R. L. Wiess and J. D. Roberts, *Biochemistry* **21**, 4916 (1982).
- ⁵⁷ X. Gao and R. Jones, *J. Am. Chem. Soc.* **109**, 3169 (1987).
- ⁵⁸ T. L. James, J. L. James and A. Lapidot, *J. Am. Chem. Soc.* **103**, 6748 (1981).
- ⁵⁹ B. Rosenburg, L. van Camp, J. E. Trosko and V. H. Mansour, *Nature (Lond.)* **222**, 385 (1969).
- ⁶⁰ J. J. Roberts and A. J. Thompson, *Prog. Nucl. Acid Res. Mol. Biol.* **22**, 71 (1979).
- ⁶¹ M. Nee and J. D. Roberts, *Biochemistry* **21**, 4920 (1982).
- ⁶² G. W. Buchanan and E. Florio, Unpublished observations.
- ⁶³ G. W. Buchanan and J. B. Stothers, *Can. J. Chem.* **60**, 787 (1982).
- ⁶⁴ L. G. Marzilli, B. de Castro, J. P. Caradonna, R. C. Stewart and C. P. Van Vuuren, *J. Am. Chem. Soc.* **102**, 916 (1980).
- ⁶⁵ G. W. Buchanan and M. J. Bell, *Mag. Res. Chem.* **24**, 493 (1986).
- ⁶⁶ C. Ramel, *Hereditas* **61**, 208 (1968).
- ⁶⁷ J. J. Mulvihill, *Science* **176**, 132 (1972).
- ⁶⁸ C. Mathew and Z. Al-Doori, *Mutat. Res.* **40**, 31 (1976).
- ⁶⁹ R. B. Simpson, *J. Am. Chem. Soc.* **86**, 2059 (1964).
- ⁷⁰ N. Juranic, R. L. Lichter, M. B. Celap, M. J. Malinar and P. N. Radivojsa, *Inorganica Chim. Acta* **62**, 131 (1982).
- ⁷¹ Y. Akiro, M. Yoshie, J. Takagi, Y. Yuzo and Y. Hideo, *Denki Tsushin Digaku Gakuho* **28**, 107 (1977).
- ⁷² N. Juranic and R. L. Lichter, *J. Am. Chem. Soc.* **105**, 406 (1983).
- ⁷³ K. Kanamori and J. D. Roberts, *Biochemistry* **22**, 2658 (1983).
- ⁷⁴ M. Blackburn, B. E. Mann, B. F. Taylor and A. F. Worrall, *Eur. J. Biochem.* **153**, 553 (1985).
- ⁷⁵ J. Mukherjee, J. I. Rogers, R. G. Khalifah and G. W. Everett, *J. Am. Chem. Soc.* **109**, 7232 (1987).
- ⁷⁶ E. R. Andrew, *Int. Rev. Phys. Chem.* **1**, 195 (1981).
- ⁷⁷ C. A. Fyfe, *Solid State NMR For Chemists*, C.F.C. Press, Guelph, Canada, (1984).
- ⁷⁸ J. R. Lyerla, C. S. Yannoni and C. A. Fyfe, *Acc. Chem. Res.* **15**, 208 (1982).
- ⁷⁹ N. M. Szerverenyl, A. Bax and G. E. Maciel, *J. Am. Chem. Soc.* **105**, 2579 (1983).
- ⁸⁰ H. H. Limbach, J. Hennig, R. Kendrick and C. S. Yannoni, *J. Am. Chem. Soc.* **106**, 4059 (1984).
- ⁸¹ B. Wehrle, H. H. Limbach, M. Koecher, O. Ermer and E. Vogel, *Angew. Chem.* **99**, 917 (1987).
- ⁸² M. Munowitz, W. W. Bachovchin, J. Herzfeld, C. M. Dobson and R. G. Griffin, *J. Am. Chem. Soc.* **104**, 1192 (1982).
- ⁸³ T.-H. Huang, W. W. Bachovchin, R. G. Griffin and C. M. Dobson, *Biochemistry* **23**, 5933 (1984).
- ⁸⁴ G. S. Harbison, J. Herzfeld and R. G. Griffin, *Biochemistry* **22**, 1 (1983).
- ⁸⁵ T. A. Cross, M. H. Frey and S. J. Opella, *J. Am. Chem. Soc.* **105**, 7471 (1983).
- ⁸⁶ M. J. Bogusky, R. A. Schiknis, G. C. Leo and S. J. Opella, *J. Mag. Res.* **72**, 186 (1987).
- ⁸⁷ G. Harbison, J. Herzfeld and R. G. Griffin, *J. Am. Chem. Soc.* **103**, 4752 (1981).
- ⁸⁸ T. H. Huang, R. P. Skarjune, R. J. Wittebort, R. G. Griffin and E. Oldfield, *J. Am. Chem. Soc.* **102**, 7377 (1980).
- ⁸⁹ R. Blinc, M. Mali, P. Oscredar, A. Prelesnir, J. Seliger and I. Zupanovic, *Chem. Phys. Lett.* **14**, 49 (1972).
- ⁹⁰ D. Schweitzer and H. W. Speiss, *J. Mag. Res.* **15**, 529 (1974).
- ⁹¹ G. S. Harbison, L. W. Jelinski, R. E. Stark, D. A. Torchia, J. Herzfeld and R. G. Griffin, *J. Mag. Res.* **60**, 79 (1984).
- ⁹² J. E. Roberts, G. S. Harbison, M. G. Munowitz, J. Herzfeld and R. G. Griffin, *J. Am. Chem. Soc.* **109**, 4163 (1987).
- ⁹³ W. H. Dawson, S. W. Kaiser, P. D. Ellis and R. R. Inners, *J. Phys. Chem.* **86**, 867 (1982).
- ⁹⁴ J. A. Ripmeester, *J. Am. Chem. Soc.* **105**, 2925 (1983).
- ⁹⁵ P. D. Majors and P. D. Ellis, *J. Am. Chem. Soc.* **109**, 1648 (1987).